Normal stresses in a shear flow of magnetorheological suspensions: viscoelastic versus Maxwell stresses

Modesto Lopez-Lopez, Pavel Kuzhir, Juan D. G. Durán, Georges Bossis

Normal stresses in a shear flow of magnetorheological suspensions: viscoelastic versus Maxwell stresses

Modesto T. López-López,[1,a)] Pavel Kuzhir,[2] Juan D. G. Durán,[1] Georges Bossis[2]

[1]Departamento de Física Aplicada, Facultad de Ciencias, Universidad de Granada, Campus de Fuentenueva, 18071 Granada, Spain

[2]Laboratoire de Physique de la Matière Condensée, CNRS UMR 6622 Université de Nice, Parc Valrose, 06108 Nice Cedex 2, France

[a)]Author to whom correspondence should be addressed; electronic mail: modesto@ugr.es

Synopsis

This work reports an experimental and theoretical study on the normal force developed by suspensions of magnetic microparticles subjected to magnetic fields. Experimental values of the normal force were obtained using a rotational rheometer, for a broad range of particle concentration in the suspensions. Applied magnetic fields up to 343 kA/m were generated in the plate-plate measuring geometry. It was found that the normal force exhibited a high-value plateau at low shear, followed by a decrease as the suspensions started to flow and a final low-value plateau at high shear. These three regions in the normal force vs. shear rate curve were well correlated with the microscopic regimes in the suspensions: field-aligned structures filling the gap; inclined structures still filling the gap; and structures non-filling the gap. The theoretical model developed is based on the equilibrium between hydrodynamic and magnetostatic torques and forces in a field-induced aggregate of particles subjected to shear. The stress tensor was obtained and the normal force calculated as the integral of the stress over the total surface of the rotational plate. A good correspondence among theoretical and experimental values was obtained.

1. Introduction

Magnetorheological (MR) fluids are suspensions of magnetizable microparticles in a liquid carrier. They present the remarkable property that their flow behavior can be reversibly tuned by adjusting the intensity of an applied magnetic field. This property is the base of many applications of MR fluids, particularly in damping systems. Detailed reviews on the preparation, characterization and applications of MR fluids are available [Ashour *et al*. (1996); Bossis *et al*. (2002); Ginder (1998); Larson (1999); Phulé (1998); Rankin *et al*. (1998)]. However, the behavior of the normal forces developed by MR fluids is a particular aspect that is not covered in the reviews. In fact, there are only a few works that report on this aspect. De Vicente *et al*. (2002) studied the normal force developed in highly-concentrated MR suspensions (solid concentration: 50 vol.%) during shear flow in a plate-plate rheometer. They found that for high enough values of the applied magnetic field their suspensions developed a positive normal force below the yield point. The normal force was negligible in the absence of deformation, but increased abruptly as the suspensions were strained, reaching a maximum at the onset of the flow. Above this point the normal force decreased very sharply, being negligible in the flow regime even for the highest magnetic field applied (29.7 kA/m). From these facts, the appearance of normal force was related by the authors to the existence of gap-spanning structures induced by the magnetic field applied, which when inclined by the shear will bring about a positive normal force as a consequence of the resulting magnetic torque. Later, See and Tanner (2003) also studied the normal force developed by MR suspensions subjected to magnetic field applied normally to the shear plane in a plate-plate rheometer. They found that, even in the absence of shear, their MR suspensions developed a non-negligible normal force. When the suspensions were sheared, the normal force decreases progressively as the shear rate was increased, but a non-negligible normal force was also measured even at the highest shear rate values. Similarly to de Vicente *et al*. (2002), these authors attributed the appearance of normal force to the formation of field-induced structures. Most recently, Laun *et al*. (2008) reported a study on the normal stress differences in MR fluids subjected to applied magnetic fields. The results of their study agree well with the work by See and Tanner (2003) and a similar explanation was given.

From the point of view of the theoretical modeling, few works have been reported that allow calculating the normal stresses in magnetic colloids. As an example, Zubarev and Iskakova (2000) developed a microstructural model for the calculation of the stress tensor of ferrofluids. In addition, Shkel and Klingenberg (1999) developed a macroscopic continuum model of electrorheological (ER) fluids and attributed the shear and normal stresses to the change in the free energy of the ER fluid upon strain application. However this model was restricted to the elastic deformation regime and small strains, and could not be adapted to MR fluids under flow (which is the most interesting case for industrial applications).

The motivation for our work was to find the reasons for the disagreement between the work by de Vicente *et al*. (2002) and these by See and Tanner (2003) and Laun *et al*. (2008), and to perform a rigorous analysis on the causes that provoke the appearance of field-induced normal forces in MR suspensions. Two main differences are found in the experimental protocols of these previous works, namely: (i) the intensity of the applied magnetic field was much larger in the works by See and Tanner (2003) and Laun *et al*. (2008) than in the work by de Vicente *et al*. (2002); (ii) the applied field was homogeneous in the latter work, whereas it was not in the other two works. The differences in field intensity does not seem to be a reasonable cause for the above-mentioned discrepancies, since the high sensibility of the normal force sensor 222-1364 Haake used by de Vicente *et al*. (2002), should have permitted measuring non-negligible values of the normal force in the absence of shear and in the flow regime, even for the low applied fields that they used. On the other hand, it seems reasonable to think that the lack of homogeneity of the applied field could cause the appearance of normal forces in magnetic liquids, and it is taken into account in the model developed in our present paper. As will be shown, our model covers the flow regime and takes into account the hydrodynamic stresses generated by particulate aggregates, as well as the magnetic stresses appearing both in quiescent and highly sheared states.

2. Experimental

Iron powder was supplied by BASF (Germany) and used without further treatment. The manufacturer indicates the following specifications: (i) chemical composition (wt%): minimum 97.5% Fe, 0.7–1.0% C;

0.7–1.0% N; 0.3–0.5% O; and (ii) density: minimum 7.5 g/cm^3. Our scanning electron microscopy (SEM) pictures show that iron particles are spherical and polydisperse, with an average diameter 930 ± 330 nm. Magnetization measurements (not shown here for brevity), performed with a Squid Quantum Design MPMS XL magnetometer at 20 ºC, showed that iron powder behaves as a soft ferromagnetic material. From the magnetization curve, saturation magnetization of 1722 ± 1 kA/m and initial (at 4 kA/m) susceptibility of 32 were obtained for the powder.

MR suspensions were prepared by dispersing proper amounts of iron powders in kerosene (Sigma-Aldrich; viscosity 2.1 mPa·s; density 0.79 g/cm^3). Aluminum stearate [molecular formula: $Al(C_{18}H_{35}O_2)_3$; technical grade; Sigma-Aldrich] was used as surfactant to avoid particle irreversible aggregation. The suspensions were homogenized by sonication and mechanical mixing.

A magnetorheometer (MCR 300 Physica-Anton Paar, Austria) was used for characterizing the MR properties of the suspensions at 25 °C. The measuring system geometry was a 20 mm diameter parallel-plate set for a gap width of 0.35 mm. The magnetorheometer MCR 300 was provided with an electromagnet that allows generating high magnetic fields in the measuring gap. We obtained the distribution of the magnetic field in the measuring gap for each given electric current in the coil by means of finite element method (FEM) simulations, performed using FEMM software package, version 4.2 [http://femm.foster-miller.net/]. As an example, Figure 1 shows results for the magnetic field strength without sample (Figure 1a) and for the normal component of the magnetic induction with sample (Figure 1b). As observed, the magnetic field generated by the magnetorheometer MCR 300 in the measuring gap is inhomogeneous, having a non negligible gradient along the radial coordinate. These results agree well with the measurements and simulations previously performed by Laun *et al*. (2008) for the similar Physica MCR501 rheometer.

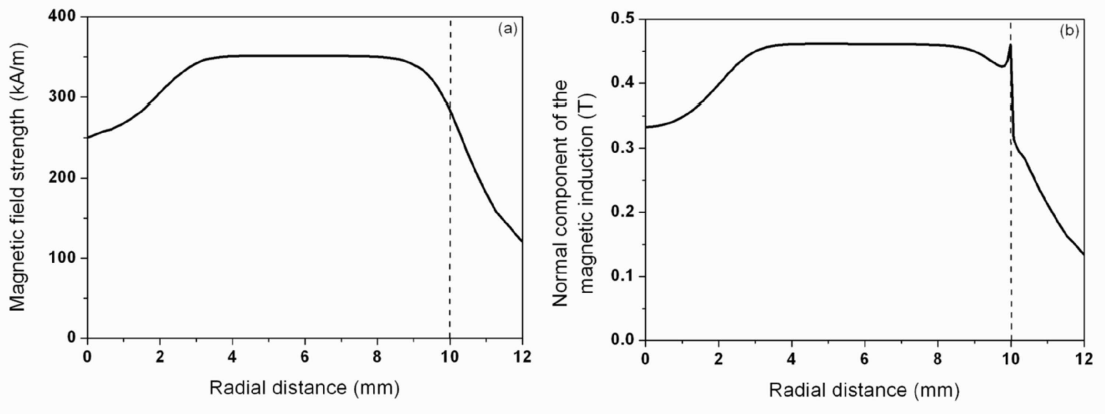

Figure 1. Calculations by means of FEM simulation of: (a) radial distribution of the magnetic field strength in the measuring gap (without sample); (b) radial distribution of the normal component of the magnetic flux density taken at the interface between the MR fluid sample (iron volume fraction, Φ=30%) and the rheometer plate in the flow regime; the electromagnet electric current considered was 2 A in both cases. The radius of the upper plate (10 mm) is indicated with a dash vertical line.

Rheological measurements were carried out as follows: (i) samples were placed between the parallel plates and initially presheared for 30 s at a large shear rate at zero magnetic field strength to ensure reproducible initial conditions; (ii) immediately afterwards, an external magnetic field (up to H_0 = 343 kAm^{-1}) was applied during a 30 s waiting time with no rate applied; (iii) finally, the samples were subjected to a shear rate ramp in the presence of the same external magnetic field strength that was used during the waiting time, and the corresponding shear stress and normal force were measured.

3. Results

We studied the response of MR suspensions containing different amounts of iron powders (between 10 and 33 vol.%) as previously described. All suspensions developed a MR response upon application of magnetic fields. Concerning the normal force, we checked that in the absence of field, the suspensions did not develop any measurable normal force. On the other hand, upon magnetic field application, a non-negligible normal force appeared in the direction of the applied field, even in the absence of shear. Obviously, in the absence of shear the existence of normal force cannot be explained in terms of the hydrodynamic stresses. Once the suspension was sheared, the normal force first diminished abruptly to a minimum as the shear rate was increased and then increased progressively to a plateau value. As an example,

the behavior for a suspension containing 10 vol.% of iron upon application of an average field of 343 kA/m is shown in Figure 2. By average field we refer here to the line integral of the field intensity along the radius of the upper plate, weighed by the radius length, obtained from curves like this shown in Figure 1a.

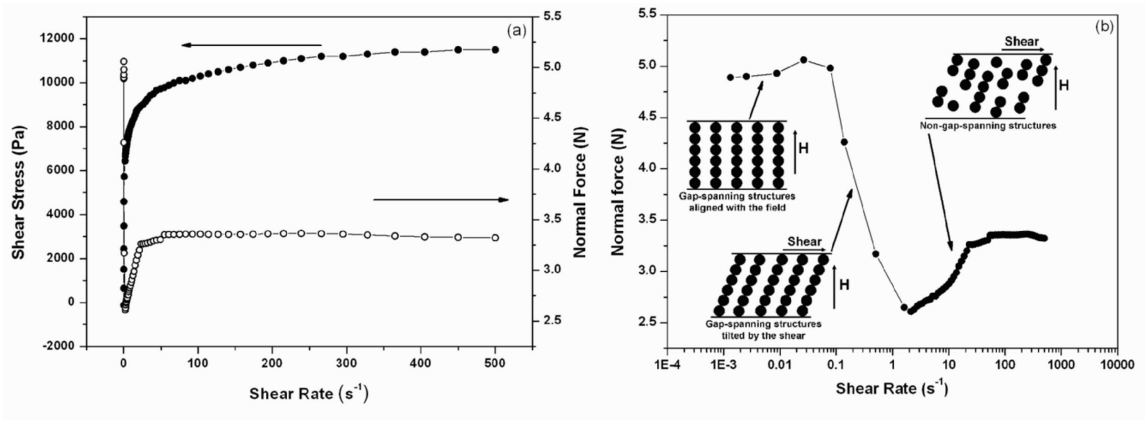

Figure 2. (a) Shear stress and normal force plotted as a function of shear rate; (b) relation between the different regimes of normal force and the expected microscopic particle structures. The solid (iron) volume fraction of the suspension is Φ=10%, and the applied field H=343kA/m.

As observed in Figure 2a, the minimum of normal force is approximately reached for a value of the shear corresponding to the start of the flow (i.e. to the yield stress). Then, the different regions of normal force could be related to the following microscopic particle structures (see Figure 2b). (i) Gap-spanning structures that are aligned in the field-direction (absence of shear or very low shear – $< 0.1\ s^{-1}$): in this region a normal force plateau is observed. (ii) Gap-spanning structures that are tilted by the effect of shear (below the yield stress): in this region the normal force diminishes as the particles structures are tilted. The maximum inclination of the particle structures before the onset of the flow could correspond to the minimum of the normal force. (iii) Non-gap-spanning structures that break by the effect of shear and rebuild by the effect of the applied field: in this region the normal force first increases with the shear and then it reaches a plateau value. These three different microscopic structures probably correspond to those identified by Claracq *et al.* (2004) in shear stress versus shear rate measurements of MR fluids.

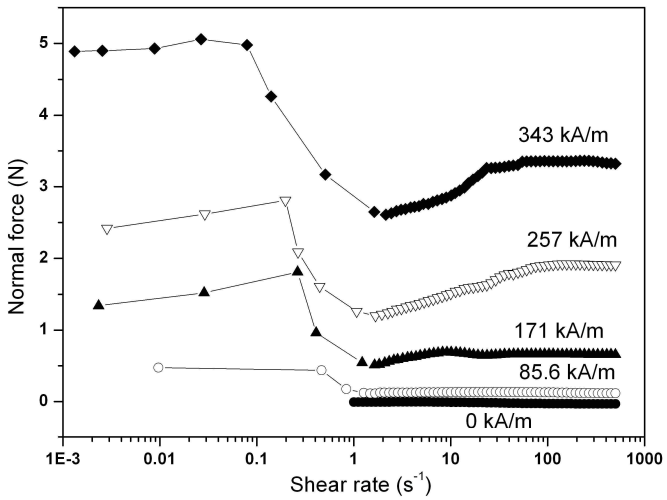

Figure 3. Normal force developed by a suspension containing 10 vol.% of iron as a function of shear rate for the indicated values of the applied field strength.

As mentioned above, we analyzed the effect of magnetic field strength on the normal force developed by the MR suspensions. As an example, in Figure 3 the values of normal force developed by a suspension containing 10 vol.% of iron, are plotted as a function of the shear rate for several values of the applied field strength. We see that the normal force in the absence of field is negligible. On the other hand, the application of a field implies the appearance of a non-negligible normal force. Concerning the effect of field strength, it is clear that the value of the normal force increases with it. However, in all cases, the curve of the normal force vs. the shear rate has a similar trend, characterized by the three different regions discussed above. Similar trends were obtained for suspensions with higher solid volume fractions, not shown here for brevity.

In order to get a clear picture about the effect of both volume fraction of solids and magnetic field strength on the normal force, we averaged the values for the high-shear plateau (flow regime). The results are plotted as a function of iron volume fraction in Figure 4. The symbols represent the experimental data, whereas the continuous lines represent fits to a parabolic function. The fact that the concentration dependence is stronger than linear could be a manifestation of the existence of hydrodynamic interactions between aggregates. At this point, it is important to mention that a quadratic dependence of the normal stress differences of ferrofluids on their volume fraction, associated to the existence of interparticle interactions, was found by Ilg *et al*. (2005) by means of theoretical simulation. Concerning the dependence on the field

strength, it seems to be higher than linear at low field, but then it tends to saturation as the field approaches that required for magnetically saturate the iron particles.

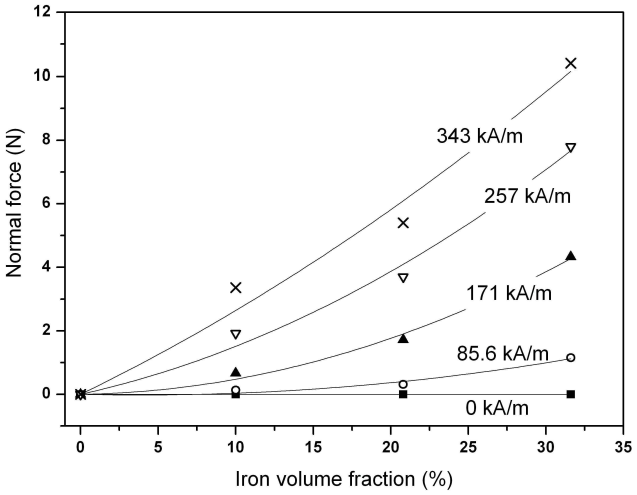

Figure 4. Normal force developed by suspensions of iron microparticles in the flow regime as a function of the iron volume fraction for the indicated values of the applied field strength. Symbols and continuous lines represent respectively the experimental data and parabolic fits.

4. Discussion: viscoelastic versus Maxwell stresses

We try in this section to develop a theoretical model that, taking into account the field inhomogeneity, allows us to explain the values of the normal force obtained in our experiments.

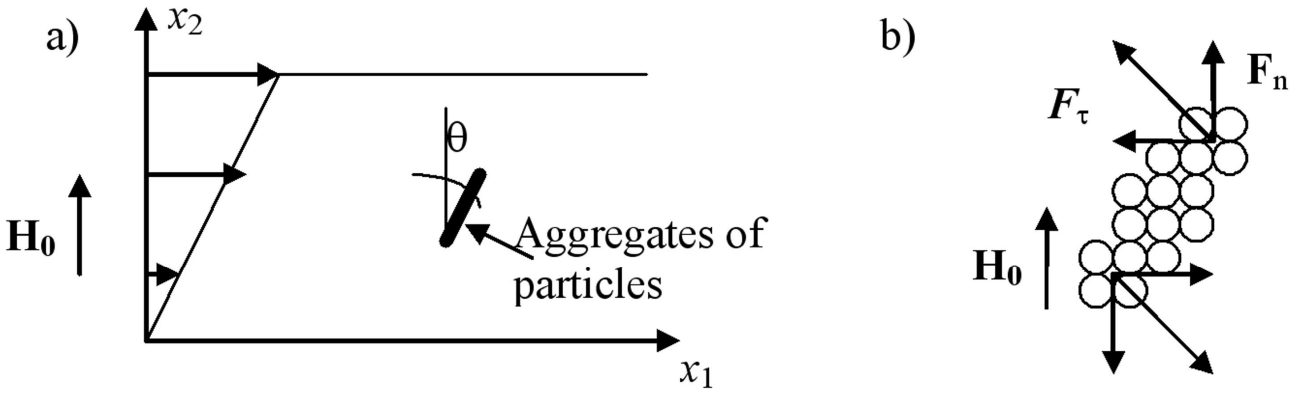

Figure 5. Simple shear flow between two infinite planes. Problem geometry is shown in figure (a); a sketch of the forces transmitted from the aggregates to the planes is shown in figure (b).

4.1. Viscoelastic response in a shear flow

Let us consider a shear flow between two parallel infinite plates induced by a motion of the upper plate while the lower one is fixed (Figure 5a). A linear velocity profile is therefore established in the reference plane x_1-x_2: $v_1 = \dot{\gamma} x_2$, with $\dot{\gamma}$ being the shear rate and x_2 the coordinate along the axis 2. An external homogeneous magnetic field of intensity, H_0, is applied perpendicular to the channel walls.

To calculate the normal stresses developed in a MR suspension subjected to such flow, we shall adapt a micromechanical model previously developed [Gómez-Ramírez *et al*. (submitted)] for the shear stress in a simple shear flow. In the presence of the magnetic field, the magnetic particles of a MR suspension form elongated aggregates aligned with the field. In a shear flow these aggregates tend to align in the flow direction. If the magnetic field is high enough, the magnetic torque exerted to the aggregates protects them from flipping, so that the aggregates do not rotate, but simply perform a translational motion in the x_1-x_2 coordinate plane with the velocity of the suspending liquid and at an angle, θ, with respect to the axis 2 (Figure 5a). The aggregates are supposed to be long cylinders, their orientation angle θ is defined by the equilibrium between the magnetic and the hydrodynamic torques exerted on them, and their aspect ratio, l, is defined by the equilibrium of the tensile hydrodynamic forces and cohesive magnetic forces:

$$\tan^2\theta = \Phi_a \frac{8M_S}{3H} \frac{2+\chi_a(1-\Phi/\Phi_a)}{\chi_a^{\,2}(1-\Phi/\Phi_a)} \frac{f^{\perp}}{f_2^{\,II}}, \qquad (1)$$

$$\frac{l^2}{\ln(2l)} = \frac{\mu_0 H^2}{\eta\dot{\gamma}} \sqrt{\frac{3\chi_a^{\,2}(1-\Phi/\Phi_a)\Phi_a}{2(2+\chi_a(1-\Phi/\Phi_a))} \frac{M_S}{H} \frac{1}{f^{\perp} f_2^{\,II}}}, \qquad (2)$$

where Φ is the volume fraction of magnetic particles in the suspension, $\Phi_a \approx 0.64$ is supposed to be the internal volume fraction of the aggregates (which are composed of densely packed spherical particles), M_S is the saturation magnetization of the magnetic particles, H is magnetic field intensity inside the MR suspension, χ_a is the magnetic susceptibility of the aggregates, η is the viscosity of a suspending liquid (kerosene), $f^{\perp} \approx f_2^{\,II} \approx 1$ are numerical coefficients that are close to unity for high aspect ratio aggregates

and $\mu_0 = 4\pi \cdot 10^{-7}$ H/m is the magnetic permeability of vacuum. The magnetic susceptibility of aggregates is defined as $\chi_a = 3\Phi_a\beta/(1-\Phi_a\beta)$, with $\beta = (\mu_p - \mu_f)/(\mu_p + 2\mu_f)$, μ_p and $\mu_f = 1$ being the relative magnetic permeability of the particles and the suspending liquid (kerosene), respectively. In the considered range of magnetic fields $H_0 < 350$ kA/m, the carbonyl iron particles have a relative magnetic permeability well above unity, so the factor β is close to unity and the susceptibility of aggregates is $\chi_a \approx 3\Phi_a/(1-\Phi_a)$. The magnetic field H inside a MR suspension sandwiched between two planes is related to the external magnetic field H_0 by: $H = H_0/\mu_{22}$. Here $\mu_{22} = \mu_{II}\cos^2\theta + \mu_\perp \sin^2\theta$ is the 22-component of the magnetic permeability tensor of the MR suspension, $\mu_{II} = 1 + (\Phi/\Phi_a)\chi_a$ and $\mu_\perp = [2 + \chi_a(1+\Phi/\Phi_a)]/[2 + \chi_a(1-\Phi/\Phi_a)]$ is the relative magnetic permeability of the MR suspension in the directions parallel and perpendicular to the aggregate axes, respectively. Knowing the aggregate's orientation (eq. 1) and aspect ratio (eq. 2), we can calculate the viscoelastic stress tensor (without pressure term) developed in the MR suspension using the following expression [Pokrovskiy (1978)]:

$$\sigma^v_{ik} = 2\eta\gamma_{ik} + \frac{\Phi}{\Phi_a}\eta\left\{4\gamma_{ik} + \frac{2l^2 f_1^{II}}{3\ln(2l)}\left[e_i e_k e_l e_m - \frac{1}{3}\delta_{ik}e_l e_m\right]\gamma_{lm}\right\} + \\ + \frac{\Phi}{2\Phi_a V_a}\{e_i e_l T_{lk} + e_k e_l T_{li} - T_{ik}\} \qquad (3)$$

Here, δ_{ik} is Kronecker delta, $\gamma_{ik} = 1/2(\partial v_i/\partial x_k + \partial v_k/\partial x_i)$ is the rate-of-strain tensor, $f_1^{II} \approx 1$ is a numerical coefficient, e_i is the projection of the unit vector **e** onto the ith axis. This vector is parallel to the longitudinal axis of the aggregates and, thus, their components are $e_1 = \sin\theta$, $e_2 = \cos\theta$ and $e_3 = 0$; V_a is the aggregate volume; $T_{ik} = -\varepsilon_{ikl}T_l$ is the tensor of the magnetic torque, T_l, applied to the aggregates, ε_{ikl} is the Levi-Civita tensor. The magnetic torque acts in the coordinate plane 1-2 and, therefore, has the only non-zero component along the axis 3, which is defined by the following expression:

$$T_3 = \frac{\chi_a{}^2(1-\Phi/\Phi_a)}{2+\chi_a(1-\Phi/\Phi_a)}\mu_0 H^2\, V_a \sin\theta\cos\theta \qquad (4)$$

If we introduce eqs. 1, 2 and 4 in the stress tensor (eq. 3), and taking into account that the shear rate is $\dot{\gamma} = dv_1/dx_2$, we get the following expressions for the shear stress, $\sigma^v{}_{12}$, normal stresses, as well as for the 1st and the 2nd normal stress differences, developed in the MR suspension under shear:

$$\sigma^v{}_{12} = \eta\dot{\gamma}\left(1+2\frac{\Phi}{\Phi_a}\right) + \frac{\Phi}{\Phi_a}\mu_0 H^2\left[\kappa\sin^2\theta\cos^2\theta + \lambda\sin\theta\cos^3\theta\right], \qquad (5)$$

$$\sigma^v{}_{11} = \frac{\Phi}{\Phi_a}\mu_0 H^2\left[\kappa\left(\sin^3\theta\cos\theta - \frac{1}{3}\sin\theta\cos\theta\right) + \lambda\sin^2\theta\cos^2\theta\right], \qquad (6)$$

$$\sigma^v{}_{22} = \frac{\Phi}{\Phi_a}\mu_0 H^2\left[\kappa\left(\cos^3\theta\sin\theta - \frac{1}{3}\sin\theta\cos\theta\right) - \lambda\sin^2\theta\cos^2\theta\right], \qquad (7)$$

$$\sigma^v{}_{33} = \frac{\Phi}{\Phi_a}\mu_0 H^2\left[-\frac{\kappa}{3}\sin\theta\cos\theta\right], \qquad (8)$$

$$N_1 \equiv \sigma^v{}_{11} - \sigma^v{}_{22} = \frac{\Phi}{\Phi_a}\mu_0 H^2\left[-\frac{1}{4}\kappa\sin(4\theta) + \frac{1}{2}\lambda\sin^2(2\theta)\right], \qquad (9)$$

$$N_2 \equiv \sigma^v{}_{22} - \sigma^v{}_{33} = \frac{\Phi}{\Phi_a}\mu_0 H^2\left[\frac{1}{2}\kappa\sin(2\theta)\cos^2\theta - \frac{1}{4}\lambda\sin^2(2\theta)\right]. \qquad (10)$$

In these formulas, $\kappa = \left(\frac{2\chi_a{}^2(1-\Phi/\Phi_a)\Phi_a}{3(2+\chi_a(1-\Phi/\Phi_a))}\frac{M_S}{H}\right)^{1/2}$ and $\lambda = \frac{\chi_a{}^2(1-\Phi/\Phi_a)}{2+\chi_a(1-\Phi/\Phi_a)}$ are dimensionless parameters and the angle θ is given by eq.(1). Note that the normal stresses appear to be independent of the shear rate. This is simply because the stresses generated by the particles are roughly proportional to the shear rate times the square of the aggregate aspect ratio ($\dot{\gamma}l^2$), and the latter decreases with the shear rate as $l^2 \propto \dot{\gamma}^{-1}$. Let us remark at this point that the aggregates are destroyed by the effect of the hydrodynamic tensile force, which is proportional to the shear rate, while they are reconstructed by the effect of the

attractive dipolar force between particles. The aggregate length (or aspect ratio) is obtained by the balance of these two forces and, therefore, it appears to be inversely proportional to the root square of the shear rate, as seen in eq. 2. However, such behavior holds within certain ranges of shear stress and magnetic fields, wherein the aggregate aspect ratio is approximately larger than ten, when the slender body theory [Batchelor (1970)] used in our model could be applied safely. A suitable dimensionless parameter that could indicate the limits of our model is the ratio of hydrodynamic to magnetic forces that is defined as the Mason number. In this work we express it as $Ma = \eta\dot{\gamma}/(\mu_0 H^{3/2} M_S^{1/2})$, but note that different expressions for this number can be found [Klingenberg *et al.* (2007)]. Using eq. 2 with a value of ten for *l*, we obtain for our experimental conditions maximum values of *Ma* ranging between 0.17 and 0.16 for particle volume fractions $0.1<\Phi<0.3$. Thus, in our experiments, this parameter remains well below 1 and our theory could be applied. Otherwise, if the shear rates attain extremely high values, corresponding to $Ma >> 1$, the aggregates would be totally destroyed by the shear flow, and the MR fluid would behave as a conventional suspension of isolated particles without any noticeable normal stress in this range of volume fraction. Thus, we expect that at $Ma > 0.17$ the normal force decreases monotonically with the shear rate up to zero at infinite shear rate. Note further that the sum of the three viscoelastic normal stresses is zero: $\sigma^v_{ii} = 0$, meaning that the viscoelastic stress tensor is traceless. Concerning the shear stress, it appears to follow a Bingham rheological law, $\sigma^v_{12} = \sigma_Y + \eta\dot{\gamma}\left(1 + 2\Phi/\Phi_a\right)$, with the yield stress defined by the second term of equation (5):

$$\sigma_Y = \frac{\Phi}{\Phi_a}\mu_0 H^2\left[\kappa \sin^2\theta\cos^2\theta + \lambda \sin\theta\cos^3\theta\right]. \qquad (10)$$

This is the dynamic yield stress, defined by extrapolation of the flow curve to zero shear rate. Notice that the viscoelastic stress tensor is not symmetric, which is the case for the fluids with applied external torques. The asymmetric part of the stress tensor is proportional to the torque tensor T_{ik}, so in our case it is equal to $\sigma^v_{12} - \sigma^v_{21} = \Phi T_3/\Phi_a V_a = (\Phi/\Phi_a)\lambda\cdot\mu_0 H^2 \sin\theta\cos\theta$.

In order to get a first analysis of our theory, we show in Figure 6 the yield stress and the normal stress differences N_1 and N_2 versus the magnetic field intensity H_0, for the particle volume fraction, $\Phi = 0.1$. All the three stresses are growing functions of the magnetic field intensity indicating that higher magnetic fields induce longer aggregates, which dissipate more energy. From the microscopic point of view, a restoring magnetic torque acts on the aggregates of the MR fluid and tends to align them with the magnetic field. Being tilted by the shear flow, the aggregates tend to turn in the counterclockwise direction and, therefore, exert forces to the surrounding liquid (Figure 5b) and the latter transmits them to the upper plane of the shear flow cell. Thus, the resulting restoring force exerted to the upper plane comes from the forces generated by each aggregate. The tangential component of this force is oriented in a direction opposite to the flow and is, therefore, responsible for the shear stress enhancement in the presence of a magnetic field (i.e. appearance of yield stress). The normal component of the resulting force pushes the upper plane upwards, which explains the origin of the viscoelastic normal stresses found in our theory. In more details, the 1st normal stress difference, N_1, is positive and appears to be approximately two times larger than the yield stress, σ_Y. The 2nd normal stress difference, N_2, is negative and its absolute value appears to be about six times lower than N_1 and about two times lower than σ_Y.

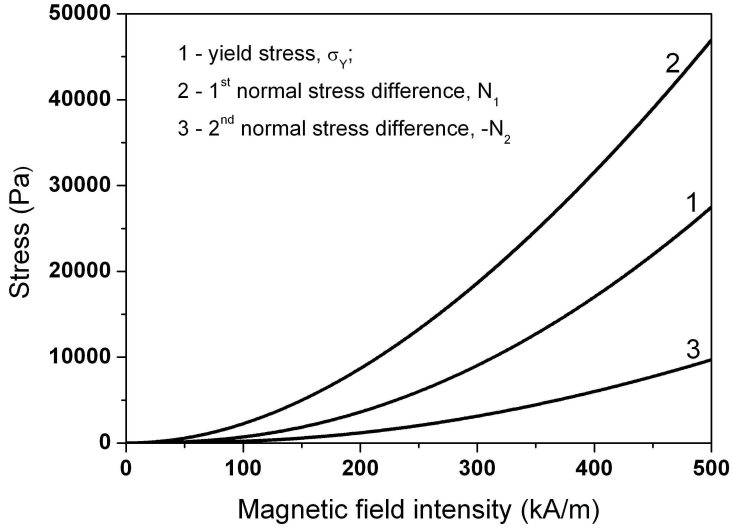

Figure 6. Theoretical dependences of the yield and normal stresses versus the intensity of the external homogeneous magnetic field, for a MR suspension containing 10 vol.% solid fraction.

At this point it is important to remark that our theory does not take into account the hydrodynamic interactions between aggregates, which, in a concentrated regime, would enhance considerably the stress and would induce Φ^2 and higher order terms in the stress tensor.

4.2. Analysis of the forces in plate-plate geometry

Now, having expressions for each component of the viscoelastic stress tensor, it is possible to calculate the normal force and the torque exerted by the MR fluid on the rotating plate of the rheometer (Figure 7).

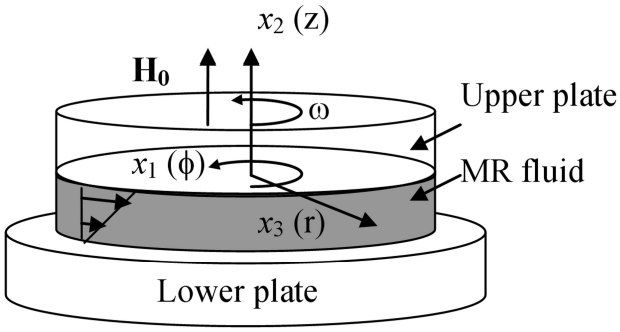

Figure 7. Sketch of the plate-plate geometry of the rheometer.

First we should determine the total stress developed in the MR fluid, which contains an isotropic pressure term, the viscoelastic term, σ^{v}_{ik}, and the Maxwell stress, σ^{M}_{ik}, which appears in any matter subject to a magnetic field:

$$\sigma = -p\delta_{ik} + \sigma^{v}{}_{ik} + \sigma^{M}{}_{ik} \qquad (11)$$

We consider here that from the point of view of the experimental geometry, the permeability of the MR fluid varies from point to point in a continuous way and, therefore, it can be calculated by using Maxwell-Garnett theory [Garnett (1904)]. Rigorously, this would impose a restriction to the aggregate size, which should be well below the rheometer gap. However, Maxwell-Garnett theory can still be used to obtain a semi-quantitative estimation of the suspension permeability for non-homogeneous suspensions, such as

suspensions of gap-spanning aggregates. Then, the Maxwell stress inside the MR fluid is defined by the same formula as for a ferrofluid [Bashtovoi *et al*. (1988); Ilg and Odenbach (2009)]:

$$\sigma^{M}{}_{ik} = -\frac{1}{2}\mu_0 H^2 \delta_{ik} + H_i B_k \,, \tag{12}$$

where **B** is the magnetic flux density in the MR fluid, which is related to the magnetic field intensity **H** and the MR fluid magnetization **M** through the relation $\mathbf{B} = \mu_0(\mathbf{H}+\mathbf{M})$. The MR fluid magnetization is related to the magnetization of each aggregate, $\mathbf{M}_a$, through the expression $\mathbf{M} = \Phi\mathbf{M}_a/\Phi_a$. Using this formula, it is easy to show that the antisymmetric part of the Maxwell stress tensor is exactly opposite to the antisymmetric part of the viscoelastic tensor:

$$(\sigma^{M}{}_{ik})_a = \frac{1}{2}\mu_0(H_i M_k - H_k M_i) = -\frac{\Phi}{2\Phi_a}\mu_0(M_{ia}H_k - M_{ka}H_i) = -\frac{\Phi}{2\Phi_a V_0}T_{ik} = -(\sigma^{v}{}_{ik})_a \tag{13}$$

Thus, the total stress (11) is symmetric, which is consistent with the conservation of the total angular momentum in the suspension. In order to calculate the force and the torque exerted by the MR fluid on the rheometer plate, we must know the pressure distribution on the plate surface. The pressure is found from the equation of motion of the MR fluid, which is simply $\nabla\cdot\sigma = 0$, when fluid inertia and gravity forces are neglected. Taking into account (11) and (12), this equation reads:

$$-\nabla p + \nabla\cdot\sigma^{v} + \mu_0\mathbf{M}\cdot\nabla\mathbf{H} = \mathbf{0} \tag{14}$$

The last term is the volume density of the magnetic force in the MR fluid in inhomogeneous magnetic fields. The sum of the pressure gradient and magnetic force terms (the 1st and the 3rd terms) can be rearranged as $-\nabla p + \mu_0\mathbf{M}\cdot\nabla\mathbf{H} = -\nabla\left(p - \mu_0\int \mathbf{M}\cdot d\mathbf{H}\right)$. And, introducing the equivalent pressure, $p^* = p - \mu_0\int \mathbf{M}\cdot d\mathbf{H}$, the equation (13) takes the following form:

$$-\nabla p^{*}+\nabla\cdot\sigma^{v}=\mathbf{0} \qquad (15)$$

The upper rotating plate drags the MR fluid, such that its velocity has only polar component $v_1 = f(x_2,x_3)$. Due to the axial symmetry of the problem, the magnetic field **H** has a zero polar component, $H_1 = 0$, and the pressure p is supposed to be independent of the polar coordinate x_1. The aggregates are supposed to be in the 1-2-coordinate plane, so that they will not give any contribution to the shear components σ^{v}_{13}, σ^{v}_{31}, σ^{v}_{23}, σ^{v}_{32}, and, thus, these will be defined only by the solvent stress. Thus, taking into account the velocity profile, $v_1 = f(x_2,x_3)$, $\sigma^{v}_{23}=\sigma^{v}_{32}=0$ and $\sigma^{v}_{13}=\sigma^{v}_{31}=\eta\partial v_1/\partial x_3$. In addition, the later stress is negligible as compared to the 12-component of the solvent stress $\sigma^{solvent}_{12}=\eta\partial v_1/\partial x_2$ and is neglected in the rheometry theory [Macosko (1994)]. The remaining components of the viscoelastic stress tensor are defined by eqs. (5)-(8). Finally, the three components of the equation of motion along the coordinate axes 1, 2 and 3 (Figure 7) will take the following form:

$$\frac{\partial\sigma^{v}_{12}}{\partial x_2}=0,\qquad \frac{\partial p^{*}}{\partial x_2}=\frac{\partial\sigma^{v}_{22}}{\partial x_2},\qquad \frac{\partial p^{*}}{\partial x_3}=\frac{\partial\sigma^{v}_{33}}{\partial x_3}-\frac{\sigma^{v}_{33}-\sigma^{v}_{11}}{x_3} \qquad (16)$$

The normal force acting on the rheometer plate is the integral of the stress over the total surface Σ of the plate:

$$F_2=\oiint_{\Sigma}\sigma_{2k}n_k dS=\oiint_{\Sigma}(-p\delta_{2k}+\sigma^{v}_{2k}+\sigma^{M}_{2k})n_k dS, \qquad (17)$$

where **n** is the unit outward vector normal to the surface. The pressure and the viscoelastic terms are zero outside of the MR fluid, so, they are integrated only over the surface of the rheometer plate wetted by the MR fluid, Σ_W. The integral of the Maxwell stress exerted on a non-magnetic rheometer plate can be presented as [Rosensweig, 1985]: $\oiint_{\Sigma}\left[\sigma^{M}_{2k}\right]n_k dS$, where $\left[\sigma^{M}_{ik}\right]$ denotes the jump of the Maxwell stress on

the surface of the plate. The latter is non-zero only along the MR fluid/plate interface, so the Maxwell stress is also integrated over the wetted surface Σ_W. The equation (17) reads now:

$$F_2 = -\iint_{\Sigma_W} \left(-p + \sigma^v{}_{22} + \left[\sigma^M{}_{22}\right] \right) dS \qquad (18)$$

According to [Bashtovoi *et al*. (1988)], the jump of the normal component of the Maxwell stress is equal to $\left[\sigma^M{}_{22}\right] = -(1/2)\mu_0 M_n{}^2$, where M_n is the component of the MR fluid magnetization normal to the rheometer plate.

Introducing the equivalent pressure p^*, and passing to the polar coordinate system (r,ϕ), equation (18) becomes:

$$F_2 = 2\pi \int_0^R r \left(p^* + \mu_0 \int \mathbf{M} \cdot d\mathbf{H} - \sigma^v{}_{22} + \frac{1}{2}\mu_0 M_n{}^2 \right) dr \qquad (19)$$

Replacing $\int r p^* dr$ by $(1/2)\int d(r^2 p^*) - (1/2)\int r^2 (\partial p^*/\partial r) dr$, performing integration by parts and using the third equation of (16), we obtain

$$F_2 = \pi R^2 \left[p^*(R) - \sigma^v{}_{33}(R) \right] + 2\pi \int_0^R r \left(\mu_0 \int \mathbf{M} \cdot d\mathbf{H} + \frac{1}{2}\mu_0 M_n{}^2 \right) dr + \pi \int_0^R r (N_1 - N_2) dr \qquad (20)$$

In order to find the first term in the right-hand side of (20), we apply a boundary condition at the edge of the MR fluid sample ($r = R$), which postulates a discontinuity of the total stress. So, neglecting capillary effects, we have: $-p(R) + \sigma^v{}_{33}(R) + \left[\sigma^M{}_{33}\right] = 0$, where $\left[\sigma^M{}_{33}\right]$ denotes the jump of the Maxwell stress on the MR fluid meniscus and is equal to $-(1/2)\mu_0 (M_n{}^2)_m$, where $(M_n)_m$ is the component of the MR fluid magnetization normal to the surface of the MR fluid meniscus. The magnitude $(M_n)_m$ must not be confounded with M_n –normal component of the magnetization at the surface of the upper plate of the rheometer. Using the equivalent pressure, the boundary condition takes its final form:

$$-p^*(R) + \left(\mu_0 \int \mathbf{M} \cdot d\mathbf{H} \right)_{r=R} + \sigma^v{}_{33}(R) - (1/2)\mu_0 \left(M_n{}^2 \right)_m = 0, \qquad (21)$$

where the subscript "$r = R$" denotes that the primitive $\int \mathbf{M} \cdot d\mathbf{H}$ is calculated at $r = R$.

Thus, substituting (21) into (20), we get the final result for the normal magnetic force:

$$F_2 = 2\pi \int_0^R r \left(\mu_0 \int_R^r \mathbf{M} \cdot d\mathbf{H} + \frac{1}{2}\mu_0 {M_n}^2 - \frac{1}{2}\mu_0 \left({M_n}^2 \right)_m \right) dr + \pi \int_0^R r(N_1 - N_2) dr \qquad (22)$$

The first integral of this equation represents the magnetic force and exists even at rest, when the suspension is not strained. The second integral stands for the pure viscoelastic response of the MR suspension under flow and has the same form as for conventional viscoelastic fluids [Macosko (1994)]. The magnetic force (first integral of eq. 22) contains three terms. The first one appears only when the magnetic field is inhomogeneous and represents the force pushing the MR fluid in the direction of the field gradient. In our experimental geometry, the magnetic field is inhomogeneous, so this term must be taken into account. The second term comes from the Maxwell stress and represents the magnetic pressure jump $\left[\sigma^M{}_{22}\right] = (1/2)\mu_0 {M_n}^2$ integrated over the wetted surface. This term appears due to the fact that the MR fluid sample tends to be stretched along the magnetic field lines, in order to decrease its magnetic energy. As a consequence of this term, even at rest, in a perfectly homogeneous magnetic field, we will always have a positive normal magnetic force equal to $(1/2)\mu_0 {M_n}^2 \pi R^2$. The third term corresponds to the jump $\left[\sigma^M{}_{33}\right]$ of the Maxwell stress on the meniscus surface, which is called magnetic pressure jump. In fact, due to the edge effects, the magnetic field becomes quite inhomogeneous in the vicinity of the MR fluid meniscus and, therefore, the magnetic field intensity and the magnetization could have a radial component.

In order to calculate both the magnetic and the viscoelastic components of the normal force, we need the magnetic field distribution inside the MR fluid sample. We obtained this distribution by FEM simulations of the Maxwell magnetostatic equations. A typical distribution of the normal component of the magnetic flux density along the wetted surface of the rheometer plate is shown in Figure 1b. With this aim, the MR fluid was considered as an anisotropic medium, with magnetic permeability components: $\mu_{22} = \mu_{II}$ and $\mu_{33} = \mu_\perp$ at rest; and $\mu_{22} = \mu_{II} \cos^2\theta + \mu_\perp \sin^2\theta$ and $\mu_{33} = \mu_\perp$ in the flow regime. Note that both $\mu_\perp$ and $\mu_{//}$ were defined above (cf. paragraph after eq. 2). At this point, it is important to remark that we will not calculate here the values corresponding to the pre-yield regime, which will remain as an open question. Nevertheless, the conclusions obtained will be general, since in our model, only the expressions of the

magnetic permeability depend on the regime considered. Appropriate expressions for the magnetic permeability of a MR suspension in the static and pre-yield regimes could be found in Volkova (1998).

Once the magnetic field distribution is known, the normal force can be calculated using eq. (22). Let us first analyze the importance the magnetic normal force (first integral of eq. 22) in the case of a MR suspension at rest, when the shear strain and shear rate are both zero. The theoretical and experimental dependencies of the magnetic normal force on the applied magnetic field strength are shown in Figure 8, for a suspension with 10% volume fraction of iron particles. As observed, there is a satisfactory correspondence between theoretical and experimental results, which confirms the importance of the Maxwell stresses in MR suspensions. Concerning the relative importance of the three terms of the magnetic force, the second term (which is due to the magnetic pressure jump on the rheometer plate –see eq. 22) is proved to be the major contribution to the total normal force. The contributions of the other two terms (which are due to the field gradient and to the magnetic pressure on the meniscus) are negative and their absolute values are, respectively, about 11% and 4 % of the total force. The negative sign of the term due to the magnetic field gradient can be explained as follows. The magnetic field intensity is lower in the central region of the MR fluid (r<4mm) than in the periphery (see Figure 1b). Therefore, being a growing function of the magnetic field, the pressure in the central region will be lower than that on the meniscus, i.e. lower than atmospheric pressure. Such depression sucks the rheometer plate downwards and creates a negative normal force.

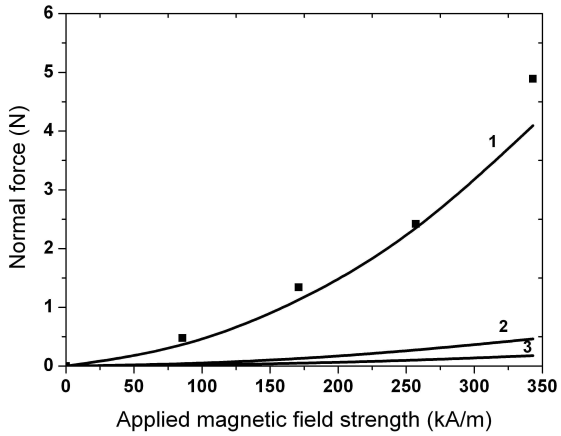

Figure 8. Normal magnetic force developed by a MR fluid (concentration 10 vol.%) at rest, plotted as a function of the applied magnetic field strength. Symbols and continuous lines represent respectively the experimental and theoretical data. Curve 1 stands for the total magnetic force. Curves 2 and 3 stand for the absolute values of the magnetic force due respectively to the field gradient and to the magnetic pressure on the meniscus.

Let us now analyze the theoretical predictions for the total normal force calculated by eq. (22). Its value is plotted in Figure 9 as a function of the magnetic field intensity -experimental results are also included for comparison. As can be seen, our theory describes semi-quantitatively the experimental results, but it underestimates the change of normal force with the volume fraction. In particular at a volume fraction 31.6%, our theory predicts a normal force rather close to the one at 20.8% whereas we observe experimentally a quite large increase. This is probably due to the fact that our theory does not take into account the hydrodynamic interactions and collisions between aggregates, which, in a concentrated regime, would enhance considerably the stress and would induce Φ^2 and higher order terms in the stress tensor. At a volume fraction 10% our model overestimates the normal force probably because the magnetic interactions between particles inside aggregates are also overestimated, and thus the aggregate length, which will give higher values of the viscoelastic stresses. Note that the viscoelastic component of the normal force, calculated by eq. (22), is about 2.7 times higher than the magnetic component for a volume fraction of particles 10%. This shows that the magnetic force is non negligible and should be taken into account, something, that to the best of our knowledge, has never been done before in a magnetorheological study.

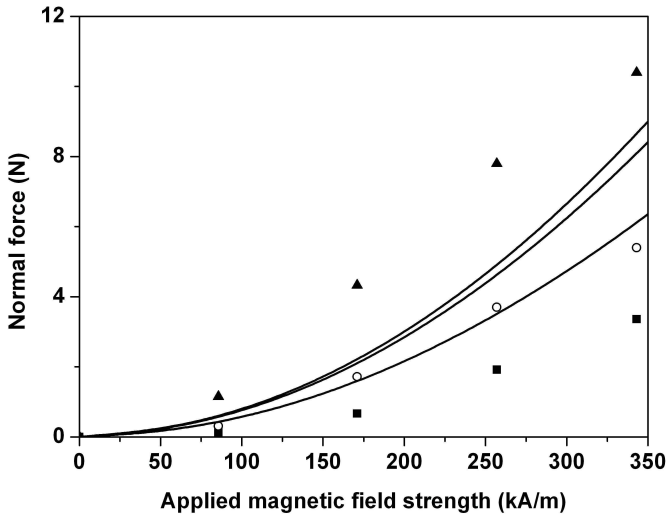

Figure 9. Normal force developed by MR suspensions in the flow regime as a function of the applied magnetic field strength. Lines and symbols represent respectively the theoretical and experimental values. Iron concentration in the MR suspensions: 10 vol.% (full squares and lower line); 20.8 vol.% (open circles and middle line); 31.6 vol.% (full triangles and upper line).

Let us now calculate the restoring torque exerted by the MR fluid onto the rheometer plate. Using the same consideration as for the normal force, the torque is given by the following relation:

$$\Gamma_2 = \Gamma_{13} = \iint_{\Sigma} (\sigma_{1k} n_k x_3 - \sigma_{3k} n_k x_1) dS = -\iint_{\Sigma_W} \left[\left(\sigma^v{}_{12} + \left[\sigma^M{}_{12} \right] \right) x_3 - \left(\sigma^v{}_{32} + \left[\sigma^M{}_{32} \right] \right) x_1 \right] dS \qquad (23)$$

As mentioned above, the 32-component of the viscoelastic stress is zero: $\sigma^v{}_{32} = 0$. Both jumps of the Maxwell stress are also zero, $\left[\sigma^M{}_{12}\right] = [H_1]B_2 = 0$ and $\left[\sigma^M{}_{32}\right] = [H_3]B_2 = 0$, because the polar component of the magnetic field intensity H_1 is zero and the jump of the radial component H_3 (tangential to the rheometer plate) is zero according to the boundary conditions for the field. Thus, eq. (23) reduces to the classical formula used in rheometry for conventional fluids [Macosko (1994)]:

$$\Gamma_2 = -2\pi \int_0^R r^2 \sigma^v{}_{12} dr \qquad (24)$$

The minus sign in this formula indicates that the restoring viscous torque is opposite to the direction of plate rotation. We see that, contrarily to the case of the normal force, the Maxwell stress does not intervene into the tangential stresses developed in a MR fluid, and only a shear viscous stress is important. In our case, we have a Bingham MR fluid with a rheological equation, $\sigma^v{}_{12} = \sigma_Y + \eta\dot{\gamma}$, where the yield stress, σ_Y, is given by eq. (10), and, thus, it is a function of the magnetic field intensity H_0(r). Therefore, it depends on the radial coordinate r, and the viscosity $\eta = \eta_0 (1 + 2\Phi / \Phi_a)$ is constant throughout the sample. Thus, the expression for the torque reads:

$$\Gamma_2 = -2\pi \int_0^R r^2 \sigma_Y dr - \frac{\pi}{2} \eta \dot{\gamma}_R R^3 = -\frac{2\pi}{3} \langle \sigma_Y \rangle R^3 - \frac{\pi}{2} \eta \dot{\gamma}_R R^3, \qquad (25)$$

where $\dot{\gamma}_R$ is the shear rate at the border of the plate ($r = R$) and $\langle \sigma_Y \rangle \equiv \frac{3}{R^3} \int_0^R r^2 \sigma_Y dr$ is the mean value of the yield stress. Let us introduce the apparent shear stress –the shear stress at the border of the plate that would appear if the considered fluid were Newtonian: $\sigma^a = \frac{2\Gamma}{\pi R^3}$. This is the shear stress measured by the rheometer. Therefore, if in experiments we observe a Bingham behavior of the MR fluid, we measure an apparent yield stress $\sigma_Y{}^a$, which is related to the real yield stress through a simple relation, $\sigma_Y{}^a = (4/3)\langle \sigma_Y \rangle$,

which can be easily deduced from eq. (25). The apparent yield stress calculated using eq. (10) is compared to the experimental one in Figure 10 for a suspension containing a volume fraction of particles 10%. We observe a semi-quantitatively agreement between the theoretical and the experimental results. However, as mentioned above, our theory does not take into account the hydrodynamic interactions between aggregates, which, in a concentrated regime, would enhance considerably the stress and, therefore, we cannot apply it safely for more concentrated suspensions.

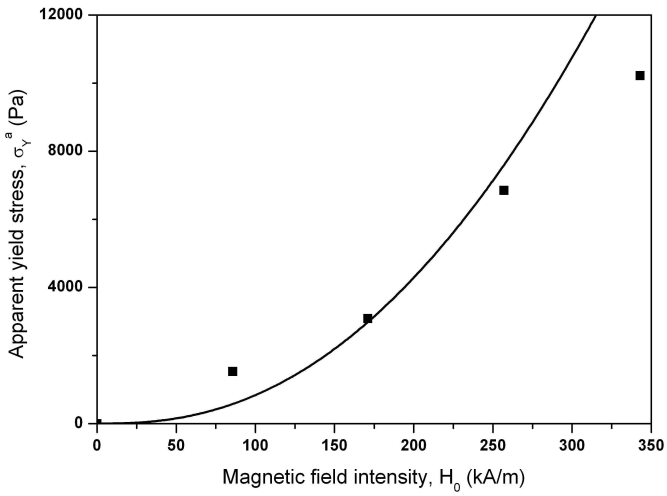

Figure 10. Apparent yield stress versus the intensity of the applied magnetic field for a suspension containing a volume fraction of particles $\Phi = 0.1$. Line and points represent theoretical and experimental values, respectively.

Note finally that, to our knowledge, among the existing theories predicting rheological behavior of MR fluids from the hydrodynamic point of view [Martin and Anderson (1996); Martin (2000); Volkova (1998); Shulman *et al*. (1986)], our theory is the first one giving a good order of magnitude for both the shear stress and the normal stress developed by a MR fluid.

5. Conclusions

We have presented in this work both an experimental and a theoretical study of the normal force developed by suspensions of magnetic microparticles (MR suspensions) in the presence of inhomogeneous magnetic fields. It has been shown that these MR suspensions develop a non-negligible normal force both in the absence and presence of shear. We can distinguish three regions in the normal force vs. shear rate curve: (i) an initial, high-value plateau that is associated to the state where the field-induced structures are not

deformed by the shear; (ii) a zone where the normal force decreases rapidly with the shear rate, which approximately coincides with the pre-yield regime, where the field-induced structures are appreciably tilted by the field, but still gap-spanning; (iii) at high shear, where structures are continuously broken by the effect of the hydrodynamic forces, a low-value plateau of the normal force is obtained. We have also analyzed the effect on normal forces of the magnetic field strength and concentration of magnetic particles in the MR suspension. We have found that the normal force increases faster than linearly both with the volume fraction and with the magnetic field in the range experimentally investigated.

In order to better explain the origin of the normal force, we have developed a theoretical model that predicts semi-quantitatively the values of this force. This model includes both the viscoelastic response of the MR fluid under an applied magnetic field and the effect of the magnetic Maxwell stress, which tends to stretch the MR fluid sample along the field lines and, thus, pushes apart the rheometer plates. In the regime of the high shear rate plateau, viscoelastic stresses and Maxwell stresses are found to give comparable contributions to the normal force. Our theory also includes the contribution to the normal stress of the radial inhomogeneity of the magnetic field, which is inherent to the kind of magnetorheometer used in this work. The results obtained indicate that for a field gradient like that shown in Figure 1 the contribution of the field inhomogeneity to the normal force is around 10 % of the total value. Nevertheless, we have ignored the possibility of particle migration due to this inhomogeneity, which would substantially change the radial distribution of the viscoelastic and magnetic normal stresses. Such migration is expected to be a long-time process, hindered by the shear flow, and therefore it should only be relevant when low viscosity carriers are used.

Acknowledgements

Projects P08-FQM-3993, P09-FQM-4787 (Junta de Andalucía, Spain), FIS2009-07321 (MICINN, Spain) and Eureka E! 3733 Hydrosmart are gratefully acknowledged for its financial support. M.T.L.-L. also acknowledges financial support by the University of Granada (Spain).

References

Ashour, O., C. A. Rogers, and W. Kordonsky, "Magnetorheological fluids: materials, characterization and devices," J. Intell. Mater. Syst. Struct. **7**, 123–130 (1996).

Bashtovoi, V. G., B. M. Berkovsky, and A. N. Vislovich, *Introduction to Thermomechanics of Magnetic Fluids* (Hemisphere Publishing Co., New York, 1988).

Batchelor G. K., "Slender-body theory for particles of arbitrary cross-section in Stokes flow," J. Fluid Mech. **44**, 419-440 (1970).

Bossis, G., O. Volkova, S. Lacis, and A. Meunier, in "Ferrofluids," *Magnetorheology: Fluids, Structures and Rheology*, edited by S. Odenbach (Springer, Berlin, 2002).

Claracq, J., J. Sarrazin, J.-P. Montfort, "Viscoelastic properties of magnetorheological fluids," Rheol. Acta **43**, 38-49 (2004).

De Vicente, J., F. González-Caballero, G. Bossis, and O. Volkova, "Normal force study in concentrated carbonyl iron magnetorheological suspensions," J. Rheol. **46**, 1295-1303 (2002).

Garnett, J.C.M., "Colours in metal phases and in metallic films," Philos. Trans. R. Soc. London **203**, 385-391 (1904).

Ginder, J. M., "Behavior of magnetorheological fluids," MRS Bull. 23, 26–29 (1998).

Gómez-Ramírez, A., P. Kuzhir, M. T. López-López, G. Bossis, A. Meunier, and J. D. G. Durán, "Steady shear flow of magnetic fiber suspensions," J. Rheol. (submitted –Manuscript # JOR-10-010).

Ilg, P., M. Kröger, and S. Hess, "Magnetoviscosity of semidilute ferrofluids and the role of dipolar interactions: Comparison of molecular simulations and dynamical mean-field theory," Phys. Rev. E **71**, 031205 (2005).

Ilg, P., and S. Odenbach, in "Colloidal Magnetic Fluids: Basics, Development and Applications of Ferrofluids," *Ferrofluid structure and rheology*, edited by S. Odenbach (Springer, Berlin, 2009).

Klingenberg, D. J., J. C. Ulicny, and M. A. Golden, "Mason numbers for magnetorheology," J. Rheol. **51**, 883-893 (2007).

Laun, J. M., C. Gabriel, and G. Schmidt, "Primary and secondary normal stress differences of a magnetorheological fluid (MRF) up to magnetic flux densities of 1 T," J. Non-Newton. Fluid Mech. **148**, 47-56 (2008).

Larson, R. G., *The Structure and Rheology of Complex Fluids* (Oxford University Press, New York, 1999).

Macosko, C. W., *Rheology: principles, measurements and applications* (VCH Publishers, New York, 1994).

Martin, J. E., and R. A. Anderson, "Chain model of electrorheology," J. Chem. Phys. **104**, 4814-4827 (1996).

Martin, J. E., "Thermal chain model of electrorheology and magnetorheology," Phys. Rev. E **63**, 011406 (2000).

Phule, P., "Synthesis of novel magnetorheological fluids," MRS Bull. **23**, 23–25 (1998).

Pokrovskiy, V. N., *Statistical mechanics of diluted suspensions* (Nauka, Moscow, 1978).

Rankin, P. J., J. M. Ginder, and D. J. Klingenberg "Electro- and magneto-rheology," Curr. Opin. Colloid Interface Sci. **3**, 373–381 (1998).

See, H., and R. Tanner, "Shear rate dependence of the normal force of a magnetorheological suspension," Rheol. Acta **42**, 166-170 (2003).

Shkel, Y. M., and D. J. Klingenberg, "A continuum approach to electrorheology," J. Rheol. **43**, 1307-1322 (1999).

Shulman, Z. P., V. I. Kordonsky, E. A. Zaltsgendler, I. V. Prokhorov, B. M. Khusid, and S. A. Demchuk, "Structure, physical properties and dynamics of magnetorheological suspensions," Int. J. Multiph. Flow **12**, 935–955 (1986).

Volkova, O., "Study of rheology of suspensions of magnetic particles," Ph.D. Thesis, Université de Nice-Sophia Antipolis, 1998.

Zubarev, A. Y., and L. Y. Iskakova, "Effect of chainlike aggregates on dynamical properties of magnetic liquids," Phys. Rev. E 61, 5415-5421 (2000).